

PACS numbers: 42.25.Bs; 78.67.Sc
DOI: 10.1070/QE2014v044n11ABEH015371

Surface polaritons in a dielectric–anisotropic nanocomposite system

D.G. Sannikov, D.I. Sementsov, L.D. Filatov

Abstract. **We have studied the peculiarities of propagation of surface polaritons at a planar interface between an isotropic dielectric and anisotropic nanocomposite with metal inclusions of ellipsoidal shape. For the case when the axes of all nanoellipsoids of revolution are perpendicular to the propagation direction and parallel to the medium interface, we have obtained frequency dependences of the propagation constant and transverse wave vector components, penetration depth and path length, longitudinal and transverse energy fluxes for surface polaritons. The shape of nanoellipsoids is shown to have an effect on the wave characteristics of surface polaritons.**

Keywords: *anisotropic nanocomposites, metal inclusions, surface polaritons.*

1. Introduction

Recent years have seen a growing interest in nanocomposite materials (NCMs), which have a number of unique properties allowing one to create new materials with desired structural, electromagnetic and optical characteristics. The NCM properties are largely determined by size, shape and ordering of nanoinclusions and by the degree of the material (matrix) volume filling by them [1–4]. In particular, by choosing properly the matrix material, the concentration and size of nanoinclusions, one can produce NCMs with a negative real part of complex permittivity and (or) permeability in a certain frequency range. Promising also is the use of NCMs with metal inclusions, having a strong linear and nonlinear dispersion of optical properties in the region of the plasmon resonance [5–10].

It is known that in the frequency region where one of the material parameters is negative, surface waves, i.e., surface polaritons (SPs), can propagate along a planar interface [11–15]. The wave field of surface polaritons is localised in the surface region whose thickness on each side of the interface is of the order of the wavelength. In anisotropic media, to which NCMs with anisotropic arrangement and shape of inclusions belong, the SP properties strongly depend on the direction of their propagation relative to the axes of anisotropy [16–23].

In this paper we study the properties of SP propagation along the planar interface between an isotropic dielectric and a NCM with an ellipsoidal shape of the metal nanoparticles used as fillers. For the same orientation of all the nanoparticles and their uniform distribution in the volume, an NCM is a uniaxial optical crystal with the effective permittivity tensor components, which depend on both the geometrical parameters of the structure and physical characteristics of nanoparticles. We have derived dispersion relations for nanoparticles of different shapes in the NCMs, constructed the frequency dependences of the SP penetration depth and the total energy fluxes carried by the SPs.

D.G. Sannikov, D.I. Sementsov, L.D. Filatov Ulyanovsk State University, ul. Tolstogo 42, 432700 Ul'yanovsk, Russia;
e-mail: sannikov-dg@yandex.ru, sementsovdi@mail.ru

Received 23 December 2013; revision received 12 May 2014
Kvantovaya Elektronika **44** (11) 1033–1038 (2014)
Translated by I.A. Ulitkin

2. Structure geometry and material parameters

Let us direct the z and x axes normally to the interface between the media and along the wave propagation direction, respectively. We assume that the permittivity ε_d of the dielectric in the frequency range in question is independent of frequency. An NCM is a non-conductive matrix with a permittivity ε_m, in a volume of which metal nanoparticles with a permittivity ε_p are uniformly distributed. The magnetic permeability of a dielectric medium (μ_d) and NCM (μ_n) in this optical range is considered frequency independent and equal to unity.

It is assumed that all the nanoparticles have the shape of ellipsoids of revolution, the same orientation and size, which is an order smaller than the wavelength. Below we will study one of the main orientations of the axes of revolution of all the nanoparticles when they coincide with the coordinate axis y lying in the plane of the interface (Fig. 1). In this case, the NCM has the properties of a uniaxial crystal and its effective permittivity is described by the diagonal tensor $\hat{\varepsilon}_{\text{eff}}$ with nonzero components $\varepsilon_{xx} = \varepsilon_{zz} = \varepsilon_{\text{eff}}^{\perp}$ and $\varepsilon_{yy} = \varepsilon_{\text{eff}}^{||}$. To describe the optical properties of the NCM, we use one of the most common models of an effective medium with nanoparticles of the same type – the Maxwell Garnett model, in which the effective permittivity of the medium is described by the expression [2, 3, 4, 16–18]

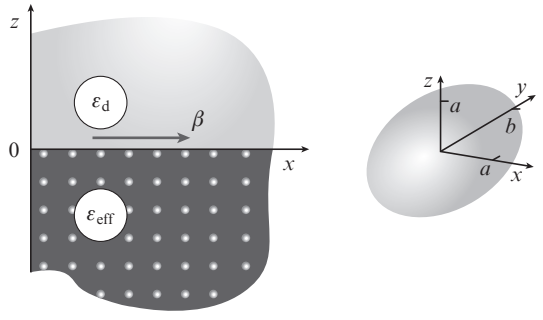

Figure 1. Geometry of the problem and shape of nanoinclusions.

$$\varepsilon_{\text{eff}}^{\perp,\parallel} = \varepsilon_{\text{m}}\left[1 + \frac{\eta(\varepsilon_{\text{p}} - \varepsilon_{\text{m}})}{\varepsilon_{\text{m}} + (1-\eta)(\varepsilon_{\text{p}} - \varepsilon_{\text{m}})g_{\perp,\parallel}}\right], \quad (1)$$

where η is the volume fraction of nanoinclusions; and $g_{\perp,\parallel}$ are the depolarising factors (or form factors), taking into account the effect of the shape of the nanoparticle on the value of the dipole moment induced on it. By neglecting absorption and frequency dispersion of the dielectric used as a composite matrix, we can consider the parameter ε_{m} to be a constant and real value. For the permittivity of metal nanoparticles we have the expression

$$\varepsilon_{\text{p}}(\omega) = \varepsilon_0 - \frac{\omega_{\text{p}}^2}{\omega^2 + \text{i}\omega\gamma}, \quad (2)$$

where ω is the frequency of light; ω_{p} is the plasma frequency; ε_0 is the contribution of the lattice; and γ is the relaxation parameter.

In the case of an ellipsoid of revolution, the depolarising factor $g_{\parallel}$ essentially depends on the inverse ratio of the lengths of the polar (a) and equatorial (b) semiaxes of nanoparticles, $\xi = b/a$. The case $\xi < 1$ corresponds to an oblate ellipsoid, for which the parameter $g_{\parallel}$ is given by the expression

$$g_{\parallel} = \frac{1}{1-\xi^2}\left(1 - \frac{\xi}{\sqrt{1-\xi^2}}\arcsin\sqrt{1-\xi^2}\right), \quad (3)$$

and the case $\xi > 1$ – to a prolate ellipsoid of revolution for which

$$g_{\parallel} = \frac{1}{\xi^2 - 1}\left[\frac{\xi}{\sqrt{\xi^2-1}}\ln(\xi + \sqrt{\xi^2 - 1}) - 1\right]. \quad (4)$$

The general relation $g_{\parallel} + 2g_{\perp} = 1$ implies that $g_{\perp} = (1 - g_{\parallel})/2$. In the case of spherical particles, $\xi = 1$, the shape anisotropy is absent and $g_{\parallel} = g_{\perp} = 1/3$.

Accounting for relaxation in expression (2) leads to integrated components of the effective permittivity, i.e., $\varepsilon_{\text{eff}} = \varepsilon'_{\text{eff}} + \text{i}\varepsilon''_{\text{eff}}$, where the real and imaginary parts are determined by the expressions:

$$\varepsilon'_{\text{eff}} = \varepsilon_{\text{m}} + \frac{\eta}{G}\left\{(\varepsilon'_{\text{p}} - \varepsilon_{\text{m}})\left[1 + g(1-\eta)\frac{\varepsilon'_{\text{p}} - \varepsilon_{\text{m}}}{\varepsilon_{\text{m}}}\right]\right.$$

$$\left. + g(1-\eta)\frac{(\varepsilon''_{\text{p}})^2}{\varepsilon_{\text{m}}}\right\}, \ \varepsilon''_{\text{eff}} = \frac{\eta\varepsilon''_{\text{p}}}{G}. \quad (5)$$

Here we have introduced the notations

$$G = \left[1 + g(1-\eta)\frac{\varepsilon'_{\text{p}} - \varepsilon_{\text{m}}}{\varepsilon_{\text{m}}}\right]^2 + \left[g(1-\eta)\frac{\varepsilon''_{\text{p}}}{\varepsilon_{\text{m}}}\right]^2,$$

$$\varepsilon'_{\text{p}} = \varepsilon_0 - \frac{\omega_{\text{p}}^2}{\omega^2 + \gamma^2}, \ \varepsilon''_{\text{p}} = \frac{\gamma\omega_{\text{p}}^2}{\omega(\omega^2 + \gamma^2)}.$$

In relations (5), indices $\perp$ and $\parallel$ are omitted in quantities $\varepsilon'_{\text{eff}}$, $\varepsilon''_{\text{eff}}$ and g.

Analysis of the expressions obtained indicates a resonance character of the functions $\varepsilon_{\text{eff}}^{\perp,\parallel}(\omega)$. The resonance frequency corresponds to maxima of the imaginary part of these functions and are determined by the expression

$$\omega_{\text{res}} \approx \sqrt{\frac{(1-\eta)g\omega_{\text{p}}^2}{\varepsilon_{\text{m}} + (1-\eta)g(\varepsilon_0 - \varepsilon_{\text{m}})} - \gamma^2}. \quad (6)$$

These frequencies are related to the plasmon resonance of nanoparticles and essentially depend on their shape and size.

3. Dispersion relation

Below we consider the case of propagation of TM-type surface polaritons in the structure (due to the absence of the magnetic response of both media TE-type polaritons cannot propagate in this structure). Taking into account the harmonic dependence of the fields on time and coordinate along the wave propagation direction, $(E_x, H_y, E_z) \propto \exp[\text{i}(\omega t - \beta x)]$, we write the expressions for the components of the wave field in the NCM:

$$\frac{\text{d}^2 H_y}{\text{d}z^2} - q_{\text{n}}^2 H_y = 0, \quad E_x = \frac{\text{i}}{k_0\varepsilon_{\text{eff}}^{\perp}}\frac{\text{d}H_y}{\text{d}z}, \quad E_z = -\frac{\beta}{k_0\varepsilon_{\text{eff}}^{\perp}}H_y, \quad (7)$$

where $k_0 = \omega/c$; c is the velocity of light in vacuum; β is the propagation constant; and

$$q_{\text{n}}^2 = \beta^2 - k_0^2\varepsilon_{\text{eff}}^{\perp}\mu_{\text{n}} \quad (8)$$

is the transverse component of the wave vector. Equations (7) and (8) for the dielectric are obtained by making a substitution $\varepsilon_{\text{eff}}^{\perp} \to \varepsilon_{\text{d}}, \mu_{\text{n}} \to \mu_{\text{d}}$ и $q_{\text{n}} \to q_{\text{d}}$.

The solution to the equations for the magnetic field component H_y with allowance for its continuity at the interface can be given in the form

$$H_y(x,z) = H_0\exp(-\text{i}\beta x)\begin{cases}\exp(-q_{\text{d}}z), & z > 0,\\ \exp(q_{\text{n}}z), & z < 0.\end{cases} \quad (9)$$

The second boundary condition for a TM polariton consists in the continuity of the tangential component of the electric field at the interface, which is equivalent to the equation:

$$\left.\frac{1}{\varepsilon_{\text{d}}}\frac{\partial H_y^{\text{d}}}{\partial z} - \frac{1}{\varepsilon_{\text{eff}}^{\perp}}\frac{\partial H_y^{\text{n}}}{\partial z}\right|_{z=0} = 0. \quad (10)$$

Equation (10) with (9) taken into account leads to a dispersion relation that relates the SP propagation constant to the material parameters of media and to the frequency:

$$\frac{q_{\text{d}}}{\varepsilon_{\text{d}}} + \frac{q_{\text{n}}}{\varepsilon_{\text{eff}}^{\perp}} = 0, \ \beta = k_0\sqrt{\frac{\mu_{\text{n}}\varepsilon_{\text{d}} - \mu_{\text{d}}\varepsilon_{\text{eff}}^{\perp}}{\varepsilon_{\text{d}}^2 - (\varepsilon_{\text{eff}}^{\perp})^2}\varepsilon_{\text{d}}\varepsilon_{\text{eff}}^{\perp}}. \quad (11)$$

Below we will analyse the situation, when we can assume that $\mu_{\text{n}} = \mu_{\text{d}} = 1$ and

$$\beta(\omega) = \frac{\omega}{c}\sqrt{\frac{\varepsilon_{\text{eff}}^{\perp}(\omega)\varepsilon_{\text{d}}}{\varepsilon_{\text{eff}}^{\perp}(\omega) + \varepsilon_{\text{d}}}}. \quad (12)$$

In the case under study, $\varepsilon_{\text{d}} > 0$; therefore, in the absence of absorption the SP existence is possible only if $\varepsilon_{\text{eff}}^{\perp} < 0$ and $|\varepsilon_{\text{eff}}^{\perp}| > \varepsilon_{\text{d}}$. We draw attention to the fact that at the chosen geometry of the problem, we need only the $\varepsilon_{\text{eff}}^{\perp}$ value, which enters the wave equation (7) and the dispersion relation (11). Therefore, in all the expressions below we omit the superscript $\perp$ by assuming $\varepsilon_{\text{eff}} \equiv \varepsilon_{\text{eff}}^{\perp}$.

In the presence of absorption in the structure the SP propagation constant and the transverse wave vector components

become complex, i.e., $\beta = \beta' - i\beta''$ and $q_j = q'_j - iq''_j$ ($j = d, n$). In this case, the SP field is determined by the expression

$$H_y(x,z) = H_0(x)\exp[-i(\beta' x \mp q''_j z)]\exp(\mp q'_j z), \qquad (13)$$

where $H_0(x) = H_0\exp(-\beta'' x)$; the sign 'minus' refers to the region $z > 0$, and the sign 'plus' – to the region $z < 0$. Real and imaginary parts of the propagation constant, which determine the phase velocity and attenuation, are given by the relations

$$\beta' = \frac{k_0}{\sqrt{2}}(\sqrt{m^2+n^2}+m)^{1/2},\ \beta'' = \frac{k_0}{\sqrt{2}}(\sqrt{m^2+n^2}-m)^{1/2},$$
$$m = \frac{\varepsilon_d(\varepsilon_d\varepsilon'_{eff}+|\varepsilon_{eff}|^2)}{(\varepsilon_d+\varepsilon'_{eff})^2+(\varepsilon''_{eff})^2},\ n = \frac{\varepsilon_d^2\varepsilon''_{eff}}{(\varepsilon_d+\varepsilon'_{eff})^2+(\varepsilon''_{eff})^2}. \qquad (14)$$

Real and imaginary parts of the transverse wave vector component of the SPs, q_j, in each medium can be represented as follows:

$$q'_{d,n} = \frac{k_0}{\sqrt{2}}(\sqrt{u_{d,n}^2+v_{d,n}^2}\mp u_{d,n})^{1/2},\ q''_{d,n} = \frac{k_0}{\sqrt{2}}(\sqrt{u_{d,n}^2+v_{d,n}^2}\mp u_{d,n})^{1/2}, \qquad (15)$$

where we introduce the notations

$$u_d = \frac{\varepsilon_d^2(\varepsilon_d+\varepsilon'_{eff})}{(\varepsilon_d+\varepsilon'_{eff})^2+(\varepsilon''_{eff})^2};\ v_d = \frac{\varepsilon_d^2\varepsilon''_{eff}}{(\varepsilon_d+\varepsilon'_{eff})^2+(\varepsilon''_{eff})^2};$$

$$u_n = \frac{(\varepsilon_d+\varepsilon'_{eff})[(\varepsilon'_{eff})^2-(\varepsilon''_{eff})^2]+2\varepsilon'_{eff}(\varepsilon''_{eff})^2}{(\varepsilon_d+\varepsilon'_{eff})^2+(\varepsilon''_{eff})^2};$$

$$v_n = \varepsilon''_{eff}\ \frac{(\varepsilon'_{eff})^2-(\varepsilon''_{eff})^2-2\varepsilon'_{eff}(\varepsilon_d+\varepsilon'_{eff})}{(\varepsilon_d+\varepsilon'_{eff})^2+(\varepsilon''_{eff})^2}.$$

It follows from the representation of the wave field (13) that the planes of the SP field amplitude constant, $\beta'' x \pm q'_{d,n} z = \text{const}$, cross the interface between the media at the angles $\mp\arctan(\beta''/q'_{d,n})$ in each of the media. The planes of the phase constant, $\beta' x \mp q''_{d,n} z = \text{const}$, cross the interface at the angles $\pm\arctan(\beta'/q''_{d,n})$.

For the SP existence, the conditions $q'_d > 0$, $q'_n > 0$ must be met, which means that the amplitude of the SP wave field should decrease exponentially with distance from the interface. Obvious physical considerations also require the fulfilment of two inequalities: $\beta' > 0$, $\beta'' > 0$, the first of which indicating the absence of the backward wave, the second – the absence of amplification in the structure.

4. Numerical analysis

In the numerical analysis we used the following NCM parameters: $\varepsilon_0 = 5$; $\omega_p = 1.36\times10^{16}$ s^{-1}; $\gamma = 3.04\times10^{13}$ s^{-1} (silver nanoinclusions) [24]; $\varepsilon_m = 2.25$ (glass matrix); volume fraction of nanoinclusions, $\eta = 1.3\times10^{-2}$; and permittivity of the dielectric, $\varepsilon_d = 1$. Figure 2 shows the frequency dependences of the real and imaginary parts of the effective permittivity $\varepsilon^{\perp}_{eff}$ obtained for an NCM with nanoinclusions in the form of oblate ellipsoids, spheres and prolate ellipsoids, i.e. at $\xi = 0.5$, 1, 5. With increasing distance from the resonance frequency, ε'_{eff} asymptotically tends to $(1-\eta)\varepsilon_m + \eta\varepsilon_0$, whereas ε''_{eff} – to zero. One can see that ε'_{eff} takes negative values in a narrow frequency range and the width of this range decreases with

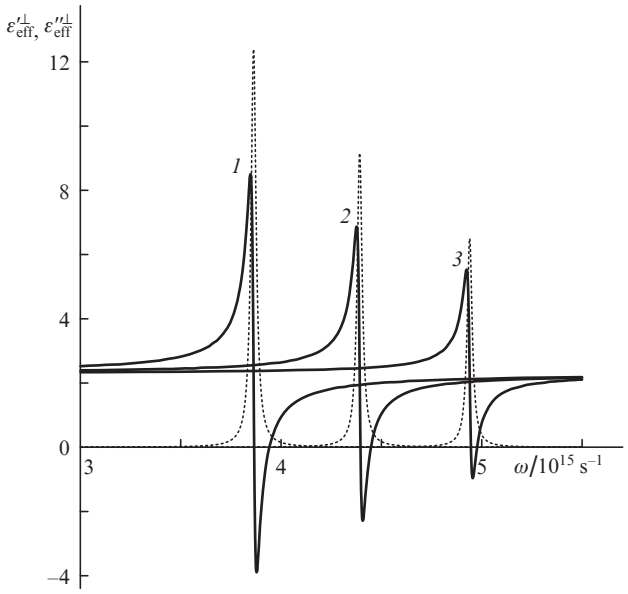

Figure 2. Frequency dependences of the real (solid curves) and imaginary (dashed curves) parts of the NCM effective permittivity $\varepsilon^{\perp}_{eff}$ at $\xi =$ (*1*) 0.5, (*2*) 1 and (*3*) 5.

increasing parameter ξ. In addition, with increasing ξ the region of the plasmon resonance shifts towards higher frequencies, and the real part of the effective permittivity and the resonance value of its imaginary part decrease.

Figure 3 shows the frequency dependences of the real and imaginary parts of the propagation constant obtained for the structure with the above NCM parameters and the dielectric material permittivity $\varepsilon_d = 1$. It is seen that the resonances of the propagation constant correspond to the resonances of the effective permittivity. The presence of losses in the structure leads to a finite value of the propagation constant in the frequency range corresponding to $\varepsilon'_{eff} < 0$, unlike a structure without absorption, for which $\beta \to \infty$ as the frequency tends to the upper boundary of the SP existence. In this case, dispersion of surface and volume polariton waves is described by

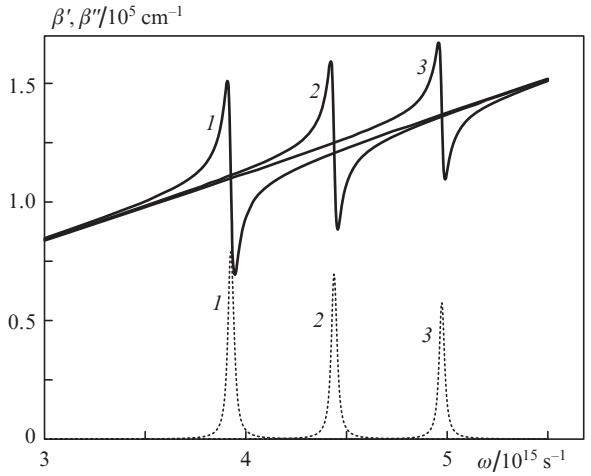

Figure 3. Frequency dependences of the real (solid curves) and imaginary (dashed curves) parts of the propagation constsnt at $\xi =$ (*1*) 0.5, (*2*) 1 and (*3*) 5.

different parts of a single continuous curve represented by the $\beta'(\omega)$ dependence. In the resonance region, the SP significantly slows down and the length of its path sharply decreases $l = (\beta'')^{-1}$, which is caused by a sharp increase in the imaginary part of the effective permittivity near the resonance frequency. In the region of a maximum growth of the $\beta'(\omega)$ value (i.e. a maximum derivative $d\beta'/d\omega$), the slowing down of the SP is most significant, and the group velocity is an order of magnitude smaller than the speed of light in vacuum. In the region where $d\beta'/d\omega < 0$, the group velocity also becomes negative. However, this frequency region corresponds to anomalous dispersion and strong absorption at which the concept of the group velocity of the wave is not always correct.

Figure 4 shows the dependences of the real and imaginary parts of the SP propagation constants on the shape of nanoinclusions, obtained for different values of the frequency ω. One can see that at a fixed frequency the dependence on the parameter ξ also has a resonant character. A substantial change in the real and imaginary parts is observed only in the resonance region, the width of which increases with increasing frequency. Away from the resonance the β' and β'' values are no longer dependent on the parameter ξ. With increasing frequency the nonresonant values of β' increase, and the β'' values tend to zero.

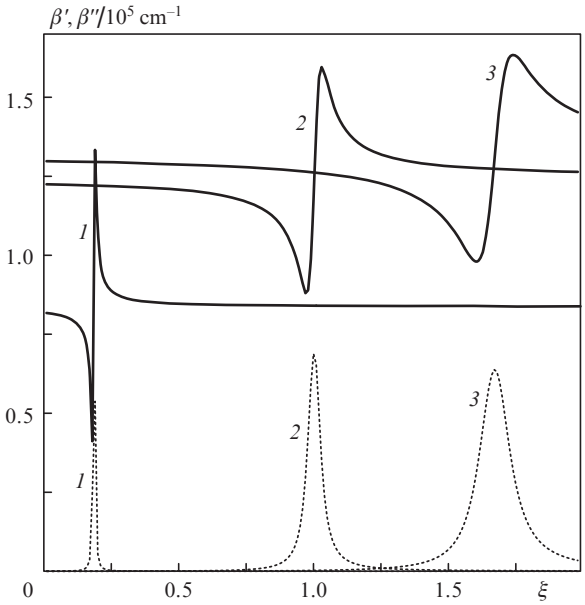

Figure 4. Dependence of the real (solid curves) and imaginary (dashed curves) parts of the SP propagation constant on the shape parameter ξ of nanoellipsoids at $\omega = (1)\ 3\times10^{15}$, $(2)\ 4.44\times10^{15}$ and $(3)\ 4.7\times10^{15}$ s^{-1}.

One of the important SP characteristics is the penetration depth of the wave field in each of the adjacent media, which is given by the expression $\lambda_{n,d} = 1/q'_{n,d}$. Figure 5 shows the dependence of the SP penetration depth into a nanocomposite and a dielectric on the frequency and shape of nanoinclusions (i.e. parameter ξ). The dependences $\lambda_{n,d}(\omega)$ are obtained for different ξ, and dependences $\lambda_{n,d}(\xi)$ – for different ω. Localisation of the radiation field near the interface of the media is maximal in those places, where the penetration depth of the surface waves is minimal: $\lambda_n \approx 3\times10^{-2}$ μm and $\lambda_d \approx 10^{-1}$ μm. Detuning from the resonance to lower frequencies causes a rapid increase in the penetration depth of the field in both a nanocomposite and a dielectric, which in the limit leads to transformation of a surface wave into a volume one. Departure from the resonance frequency to higher frequencies causes a deeper penetration of SPs into the dielectric and a relatively slow growth of λ_n in the nanocomposite. Thus, the greatest degree of the field localisation can be achieved by tuning the operating frequency. The shape of nanoinclusions also significantly affects the values of λ_d and λ_n. The wave field at selected frequencies has the highest localisation when $\xi \leqslant 0.5$, i.e., the NCM with the inclusions having the shape of oblate ellipsoids. In general, at a fixed ξ, the value of λ_d is larger than λ_n.

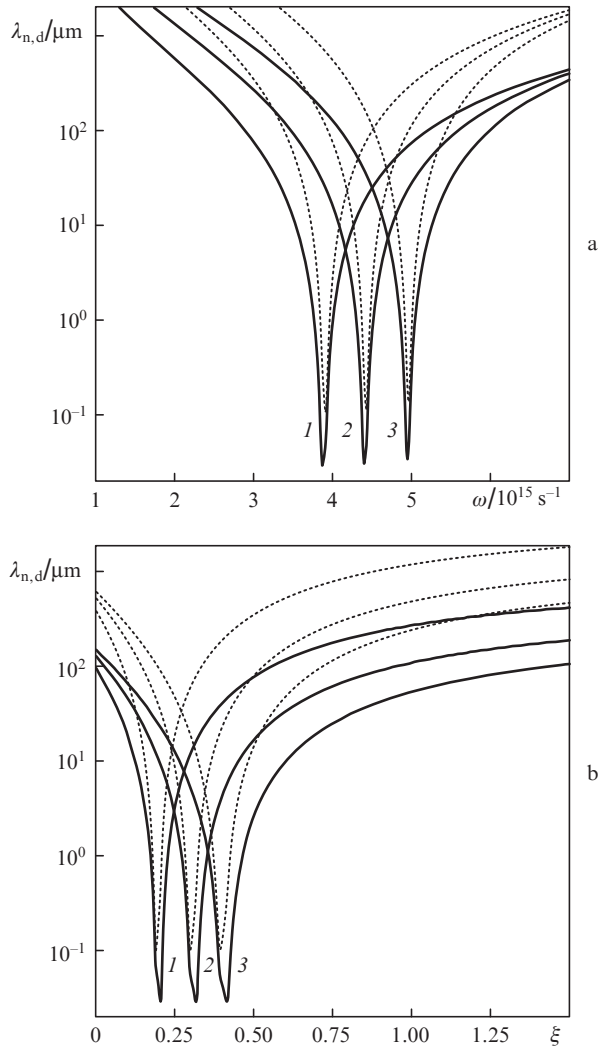

Figure 5. Dependences of the SP penetration depth into a nanocomposite (solid lines) and a dielectric (dashed curves) on (a) the frequency at $\xi = (1)\ 0.5$, $(2)\ 1$ and $(3)\ 5$ and (b) the shape of the nanoparticles in the NCM at $\omega = (1)\ 3\times10^{15}$, $(2)\ 3.44\times10^{15}$ and $(3)\ 3.7\times10^{15}$ s^{-1}.

5. Energy fluxes

An energy characteristic of the wave process in view of its harmonic function of time is the Poynting vector $\langle \boldsymbol{S} \rangle = (c/8\pi)\,\mathrm{Re}(\boldsymbol{E}\times\boldsymbol{H}^*)$, which defines in our case the period-averaged energy flux density of SPs. The presence of both a transverse and a longitudinal wave component of an electric field leads to the fact that the vector $\langle \boldsymbol{S} \rangle$ has both a longitudinal ($\langle S_x \rangle$)

and a transverse ($\langle S_y \rangle$) component. Using the relations derived for the wave fields, we can write expressions for their corresponding components of the Poynting vector:

$$\langle S_x(x,z)\rangle = \frac{cH_0^2}{8\pi k_0} \times \exp(-2\beta'' x)\begin{cases} \beta'\varepsilon_{\rm d}^{-1}\exp(-2q'_{\rm d}\, z), & z>0, \\ \dfrac{\varepsilon'_{\rm eff}\,\beta' - \varepsilon''_{\rm eff}\,\beta''}{|\varepsilon_{\rm eff}|^2}\exp(2q'_{\rm n}\, z), & z<0, \end{cases}$$

$$\langle S_z(x,z)\rangle = -\frac{cH_0^2}{8\pi k_0} \times \exp(-2\beta'' x)\begin{cases} q''_{\rm d}\,\varepsilon_{\rm d}^{-1}\exp(-2q'_{\rm d}\, z), & z>0, \\ \dfrac{\varepsilon'_{\rm eff}\,q''_{\rm n} + \varepsilon''_{\rm eff}\,q'_{\rm n}}{|\varepsilon_{\rm eff}|^2}\exp(2q'_{\rm n}\, z), & z<0. \end{cases}$$

Figure 6 shows the dependences of the longitudinal and transverse components of the SP energy fluxes on the z coordinate. The dependences are obtained for the case of spherical nanoinclusions ($\xi = 1$) at different frequencies ω. Note that at $\omega = 4.44\times10^{15}$ s^{-1} [curve (*2*)] in a narrow surface region of the nanocomposite the energy flux $\langle S_x \rangle$ is negative (see the inset in Fig. 6). The magnitude of the longitudinal energy flux in the dielectric is much larger than in the nanocomposite. This means that the total longitudinal energy flux in the structure is always positive. The transverse energy flux component $\langle S_z \rangle$ in both media is negative, i.e., the excess energy from the dielectric is transferred to the energy deficient NCM. Then, energy is partially converted into heat in the NCM. This situation is analogous to the behaviour of the surface TM wave energy flux in a semi-finite metal–dielectric system [25] and in a waveguide containing a metal substrate with a negative effective permittivity [26].

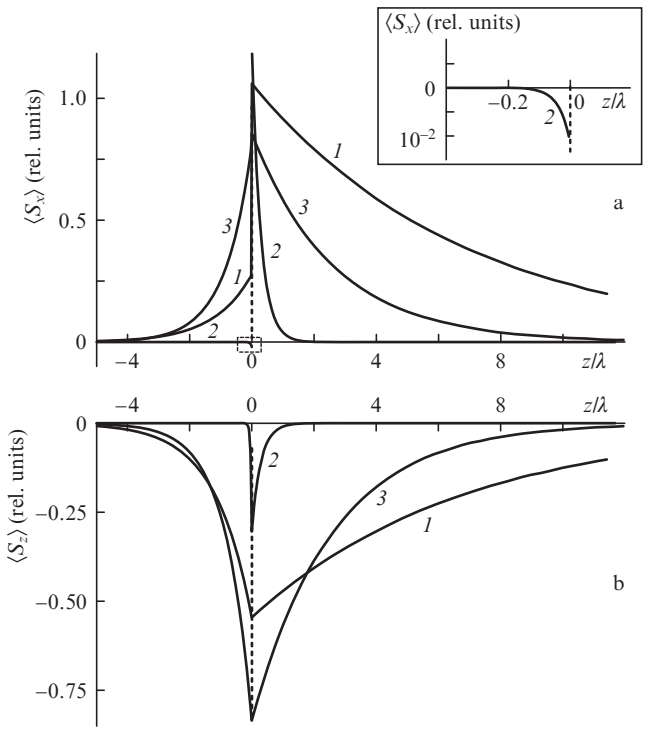

Figure 6. Dependences of (a) the longitudinal and (b) transverse components of the SP energy flux on the normalised coordinate z/λ for ω = (*1*) 3×10^{15}, (*2*) 4.44×10^{15} and (*3*) 4.7×10^{15} s^{-1} at $\xi = 1$.

Figure 7 shows the dependences of the longitudinal and transverse components of the SP energy flux in the NCM and dielectric on the shape of nanoinclusions (i.e. parameter ξ), obtained at different frequencies ω. One can see that the longitudinal component $\langle S_x \rangle$ in the dielectric is always positive, whereas in the NCM it can be both positive and negative. In this case, the region, where $\langle S_x \rangle$ is negative, shifts to larger values of ξ with increasing frequency. The component $\langle S_z \rangle$ is negative in both media. For each frequency there is a region of the parameter ξ, where the behaviour of the flux component has a resonant character. With increasing frequency, the region shifts to larger values of ξ. Because of strong absorption in the NCM in the region of the negative values of the longitudinal component the transverse component of the energy flux reaches a minimum. It is essential that in the resonance region, both components of the energy flux in each of the media are sensitive to relatively small changes in the parameter ξ.

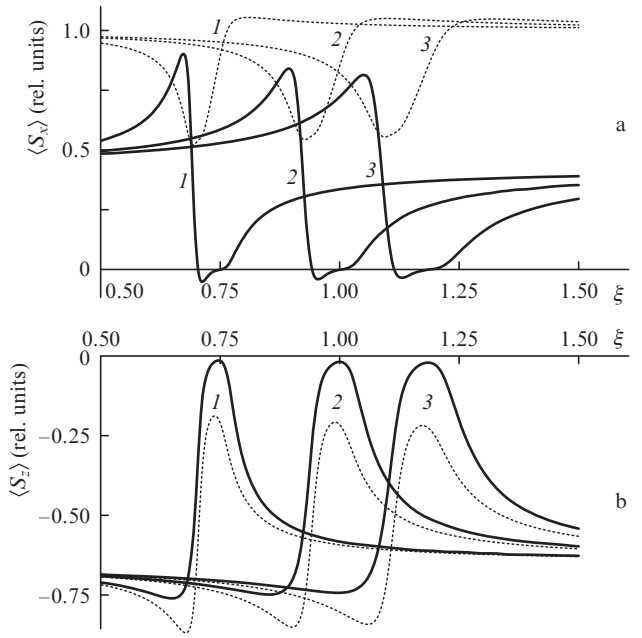

Figure 7. Dependences of (a) the longitudinal and (b) transverse components of the SP energy flux density in the NCM (solid curves) and dielectric (dashed curves) on the shape parameter of nanoparticles at ω = (*1*) 4.2×10^{15}, (*2*) 4.4×10^{15} and (*3*) 4.5×10^{15} s^{-1}.

6. Conclusions

The analysis of the peculiarities of propagation of SPs in an anisotropic structure 'dielectric–nanocomposite' with metal inclusions refers to the case where the permittivity of one of the media is complex and the structure is characterised by absorption. Allowance for absorption leads to a modification of the well-known conditions for the SP existence and the corresponding dispersion dependences. Unlike the structure with real material parameters for which the frequency spectrum has a frequency gap between the regions of existence of surface and volume waves, in the case under study the specified gap is absent, the division into surface and volume waves is

conditional and can be carried out only with respect to the depth of penetration. We have studied the case when the axes of all the ellipsoids are parallel to the interface between the media and perpendicular to the direction of SP propagation. In this case, the dispersion relation and expression for the wave fields include only the value of $\varepsilon_{\text{eff}}^{\perp}$, which makes the structure single resonant and greatly simplifies the analysis. Meanwhile, of interest are also two other major orientations of the axes of the ellipsoids – perpendicular to the interface and along the direction of propagation. In these cases, the SP behaviour will be determined by two components of the NCM effective permittivity tensor – $\varepsilon_{\text{eff}}^{\perp}$ and $\varepsilon_{\text{eff}}^{\parallel}$; therefore, the structure will exhibit two resonances, which should lead to a greater variety of the SP properties.

Note also that in an anisotropic structure SPs can be of two types. The SPs discussed in this paper are of dispersion type. This type of surface waves arises at the interface between media with different signs of permeabilities, having, as a rule, the frequency dispersion [11, 12]. The second type includes surface waves arising from the optical anisotropy of one of the boundary media at positive values of their permeabilities and relatively low frequency dispersion [17, 18]. This type of surface waves in anisotropic nanocomposites has not yet been investigated, although the nanocomposites are well-controlled media for the observation of such waves. The importance of the study of SPs in such structures consists in the applicability of the latter in the development of highly efficient devices for controlling optical and IR radiation (e.g., modulators and filters).

Acknowledgements. This work was partially supported by the Ministry of Education and Science of the Russian Federation (Contract No. 3.175.2014K) and the Russian Foundation for Basic Research (Grant No. 13-02-97026 r_povolzh'e_a).

References

1. Engheta N., Ziolkowski R.W. *Metamaterials: Physics and Engineering Explorations* (Wiley–IEEE Press, 2006).
2. Golovan' L.A., Timoshenko V.Yu., Kashkarov P.K. *Usp. Fiz. Nauk*, **177**, 619 (2007).
3. Cai W., Shalaev V. *Optical Metamaterials: Fundamentals and Applications* (New York: Springer, 2010).
4. Shalaev V.M. *Nat. Photonics*, **1**, 41 (2007).
5. Moroz A. *J. Opt. Soc. Am. B*, **26**, 517 (2009).
6. Rasnyanskii A.I., Palpant B., Debrus S., et al. *Fiz. Tverd. Tela*, **51**, 52 (2009).
7. Klimov V.V. *Nanoplazmonika* (Nanoplasmonics) (Moscow: Fizmatlit, 2010).
8. Sukhov S.V. *Kvantovaya Elektron.*, **35**, 741 (2005) [*Quantum Electron.*, **35**, 741 (2005)].
9. Vetrov S.Ya., Avdeeva A.Yu., Timofeev I.V. *Zh. Eksp. Teor. Fiz.*, **140**, 871 (2011).
10. Moiseev S.G., Ostatochnikov V.A., Sementsov D.I. *Kvantovaya Elektron.*, **42**, 557 (2012) [*Quantum Electron.*, **42**, 557 (2012)].
11. Agranovich V.M., Mills D.L. (Eds) *Surface Polaritons* (Amsterdam: North-Holland, 1982; Moscow: Nauka, 1985).
12. Dmitruk N.L., Litovchenko V.G., Strizhevskii V.L. *Poverkhnostnye polyaritony v poluprovodnikakh i dielektrikakh* (Surface Polaritons in Semiconductors and Dielectrics) (Kiev: Naukova Dumka, 1989).
13. Novotny L., Hecht B. *Principles of Nanooptics* (Cambridge: Cambridge University press, 2006; Moscow: Fizmatlit, 2009).
14. Zuev V.S., Leontovich A.M., Lidskii V.V. *Pis'ma Zh. Eksp. Teor. Fiz.*, **91**, 126 (2010).
15. Basharin A.A., Men'shikh N.L. *Pis'ma Zh. Eksp. Teor. Fiz.*, **93**, 770 (2011).
16. Knoesen A., Moharam M.G., Gaylord T.K. *Appl. Phys. B*, **38**, 171 (1985).
17. D'yakonov M.I. *Zh. Eksp. Teor. Fiz.*, **94**, 119 (1988).
18. Al'shits V.I., Lyubimov V.N. *Fiz. Tverd. Tela*, **44**, 371; 1895 (2002).
19. Abdulhalim I. *J. Opt. A: Pure Appl. Opt.*, **11**, 015002 (2009).
20. Averkov Y.O., Yakovenko V.M. *J. Opt. Soc. Am. B*, **28**, 155 (2011).
21. Baranov D.G., Vinogradov A.P., Simovski C.R. *Metamaterials*, **6**, 70 (2012).
22. Sannikov D.G., Sementsov D.I. *Fiz. Tverd. Tela*, **55**, 2209 (2013).
23. Baranov D.G., Vinogradov A.P., Simovski C.R., Nefedov I., Tret'yakov S.A. *Zh. Eksp. Teor. Fiz.*, **141**, 650 (2014).
24. Moiseev S.G. *Appl. Phys. A*, **103**, 619; 775 (2011).
25. Adams M.J. *An Introduction to Optical Waveguides* (New York: Wiley, 1981; Moscow: Mir, 1984).
26. Sannikov D.G., Sementsov D.I. *Radiotekh. Elektron.*, **49**, 1192 (2004).